17th Brazilian Congress of Thermal Sciences and Engineering
November 25th-28th, 2018, Águas de Lindóia, SP, Brazil

ENCIT-2018-0005
POLLUTANTS PREDICTION IN PULSED DIFFUSE FLAME THROUGH NUMERICAL METHOD

Antonio Marcos Feitosa da Silva
State University of Maranhao, Cidade Universitária Paulo VI, Tiririca – ZIP: 65055000 – São Luís/MA
antoniomarcos_engmecanica@ig.com.br

Maílson de Sousa Silva
State University of Maranhao, Cidade Universitária Paulo VI, Tiririca – ZIP: 65055000 – São Luís/MA
mailsonsousa00@gmail.com

Marcos Antonio Feitosa da Silva
State University of Maranhao, Cidade Universitária Paulo VI, Tiririca – ZIP: 65055000 – São Luís/MA
marcos.venci@hotmail.com

Fernando Lima de Oliveira
State University of Maranhao, Cidade Universitária Paulo VI, Tiririca – ZIP: 65055000 – São Luís/MA
fernandolima@cct.uema.br

Abstract. *Pulse Combustion is the burning process where temperature, pressure or other state variables change over time, presenting a higher mixing ratio between the fuel and the oxidant. This work proposes to numerically determine the utilized fractions in the combustion and soot emissions from this process. An experimental arrangement was made with a free burner, ie, without flame confinement. The fuel used is liquefied petroleum gas (LPG), where it is acoustically excited by a speaker. Through the experimental method, was determined the resonance frequencies in which the LPG gas was acoustically excited, at an inlet pressure of 0.5Kgf/cm² (49033.3Pa) and a mass flow rate of 0.22g/s. Under these operational conditions, the burner produced a flame with higher thermal efficiency and low soot emission. It can be affirmed that acoustic excitation reduces the emission of soot.*

Keywords: *pulsed flames, soot, acoustic excitation, numerical predictions.*

1. INTRODUCTION

Non-renewable resources such as fossil fuels are still widely used in industries despite the existence of numerous clean alternative energy sources. One of the main reasons why the use of fossil fuels is still due to its high calorific power compared to other alternative energy sources. However, the use of these conventional sources of energy causes the reduction of the ozone layer, global warming by the emission of CO2 and the release of NOx, which contributes to the formation of acid rain (Bowman, 1992).

It is relevant to optimize existing processes that minimize emission of pollutants (soot, O2, CO, CO2, NO2 and NOx gases) with low investments and operational costs. In this scenario, pulse combustion is shown as a possibility to conciliate the growing demands of the industry that uses combustion as source of thermal energy with the new environmental requirements.

Pulsed combustion is a burning process where the temperature, pressure, or other state variables varies with time, producing a turbulent mixing rate between fuel and oxidant in the flame region, making the burning process more efficient (Zinn, 1986).

Investigations have shown that pulsed combustion reduces the emissions of gaseous pollutants from partial oxidation and particulates, also promoting the increase of the convective heat transfer in the combustor (Carvalho, 1987). The resulting flames from the pulsed combustion have visually presented an aspect with less luminosity, blue colored and soot reduction (Bastos, 2001).

In recent studies, numerical simulations based on Computational Fluid Dynamics (CFD) methods are complementary to studies of combustion processes for furnaces and burners in industrial scale.

In this research is performed a diffusive flame analysis with acoustically excited mixture, being utilized numerical and experimental methods for the solution of physical problems, in order to determine the resultant fractions from the combustion.

2. EXPERIMENTAL ASSEMBLY

A free burner which there is no confinement of the flame was used to perform the experiment. The fuel used is the LPG gas, being acoustically excited by audio transducer attached radially to the burner body, at a distance of 0,155m from the gas injection. The installation of this device allows the excitation of the acoustic modes of the burner with minimum power demand by the assembly.

The burner shown in Figure 1 has a fuel inlet of 0.0045m in diameter that allows the gas to be injected into the burner body, which has internal diameter of 0.017m and 0.32m length.

The LPG gas flow in the burner body has Reynolds number equal to 1006 and Mach $3.4 \cdot 10^{-4}$, characterizing the flow in laminar and incompressible. The gas is conducted to the central region of the burner tube outlet, on which was fitted a disc for flame anchoring.

Figure 1**.** Configuration of the burner
a) speaker, b) LPG inlet, c) anchoring disc

Figure 1c shows the burner outlet where the dimension of flame's anchor disc is 0.0115m in diameter.

2.1 Analitical determination of burner's acoustic modes

The studies of confined waves - such as sound waves in a tube - demonstrate that there are certain frequencies for which superposition results in a stationary vibration pattern (Tipler, 2012). This way, the oscillation modes are formed by nodes and antinodes, in which they can behave as a closed–open tube (1/4 wave) or open-open (1/2 wave).

The resonance frequencies were calculated based on the propagation velocity of a sound wave, according to equation 1.

$$v = \sqrt{\frac{\gamma RT}{M}} \tag{1}$$

Where: T is the temperature given in absolute scale [K]; R is the universal ideal gas constant [8.314J/mol K]; M is the molar mass of the gas [0.029kg/mol]; γ the constant that depends on the type of gas, for diatomic molecules [1,4].

The uncertainties were calculated by equation 2, where σv is the standard deviation related to velocity [m/s]; σT is the standard deviation related to temperature [K].

$$\sigma_v^2 = \left(\frac{\partial v}{\partial T}\right)^2 \sigma_T^2 = \left(\frac{1}{2}\left(\frac{\gamma RT}{M}\right)^{-\frac{1}{2}}\left(\frac{\gamma R}{M}\right)\sigma T\right)^2 \tag{2}$$

The propagation velocity of sound wave was determined by substituting the measured value of the temperature in Equation 1 and corrected the uncertainties in Equation 2. The results of the velocities and the relative errors are presented in Table 1.

Table 1. Speed of sound and relative errors

Temperature measurements	Temperature (K)	Uncertainties for temperature (± K)	Speed of sound (m/s)	Uncertainties for speed of sound (± m/s)
1	302,0	1,0	348,2	0,6
2	302,0	1,0	348,2	0,6
3	297,0	1,0	345,3	0,6
4	296,0	1,0	344,7	0,6
Mean	**299,3**	**1,0**	**346,6**	**0,6**

In the open tube at both ends the air is free to travel in the displacement antinodes, being the fundamental wavelength 2 times the length of the tube and the natural frequencies are calculated by Equation 3:

$$f_n = \frac{v}{\lambda_n} = \frac{nv}{2L} = nf; \text{ where n =1,2,3...} \quad (3)$$

According to Tipler (2012), in the case of an open tube, there is a pressure node near each end. Considering that the sound wave in the tube is a one-dimensional wave - a valid hypothesis for a tube diameter much smaller than the wavelength - the pressure node is very close to the open end of the tube. For this reason there is a need to make a correction on the pipe length (ΔL). Therefore, the effective length of the tube is given by Equation 4.

$$L_{ef} = L + \Delta L \quad (4)$$

Where: L_{ef} is the effective tube length [m]; L is the tube length [m]; ΔL correction of tube ends [m].

2.2 Experimental determination of burner's acoustic modes

The procedure of sound pressure level measurement was performed according to ISO-3744: 1994 and ISO-3746: 1995 guidelines, in which a scan was performed using a *Brüel & Kjaer* 2260 *Investigator* 30-band 1/3-octave spectrum analyzer. The meter was set at 1.28m height and microphone positioned at the distance 0.01m from the burner anchor, as shown in Figure 2.

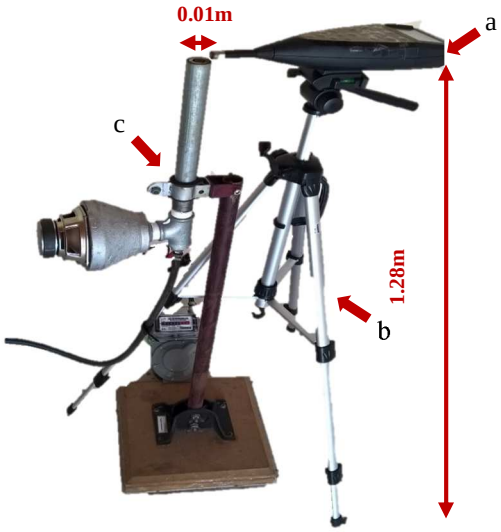

Figure 2. Experimental arrange for frequency measurements
a) *Brüel & Kjaer* 2260 *Investigator* b) support, c) burner's assembly

2.3 Numerical method of the combustion

For the elaboration of the numerical model, first was designed the real scale geometric model in CAD platform. Additionally, a combustion chamber (Figure 3c) was adapted to the geometry, with the following dimensions: larger diameter of 0.09m; smaller diameter of 0.03m; neck length of 0.06m; overall length of 0.450m. The creation of this geometry allowed the computational domain to be extended up to the height of the flame, allowing its analysis, as shown in Figure 3.

Figure 3. Geometric model of the burner
a) Diffuser, b) burner's body, c) combustion chamber

3. RESULTS AND DISCUSSIONS

In order to define the acoustic behavior of the open-burner, it was necessary to determine the modes of the resonance frequencies by analytical method, through the application of equations 1, 2, 3 and 4, and verified by the experimental method.

The graph of Figure 4 shows the seven first harmonics of resonance frequencies of the burner body. At those frequencies, the burner presents better thermal efficiency, with reduction in the amount of pollutants emission.

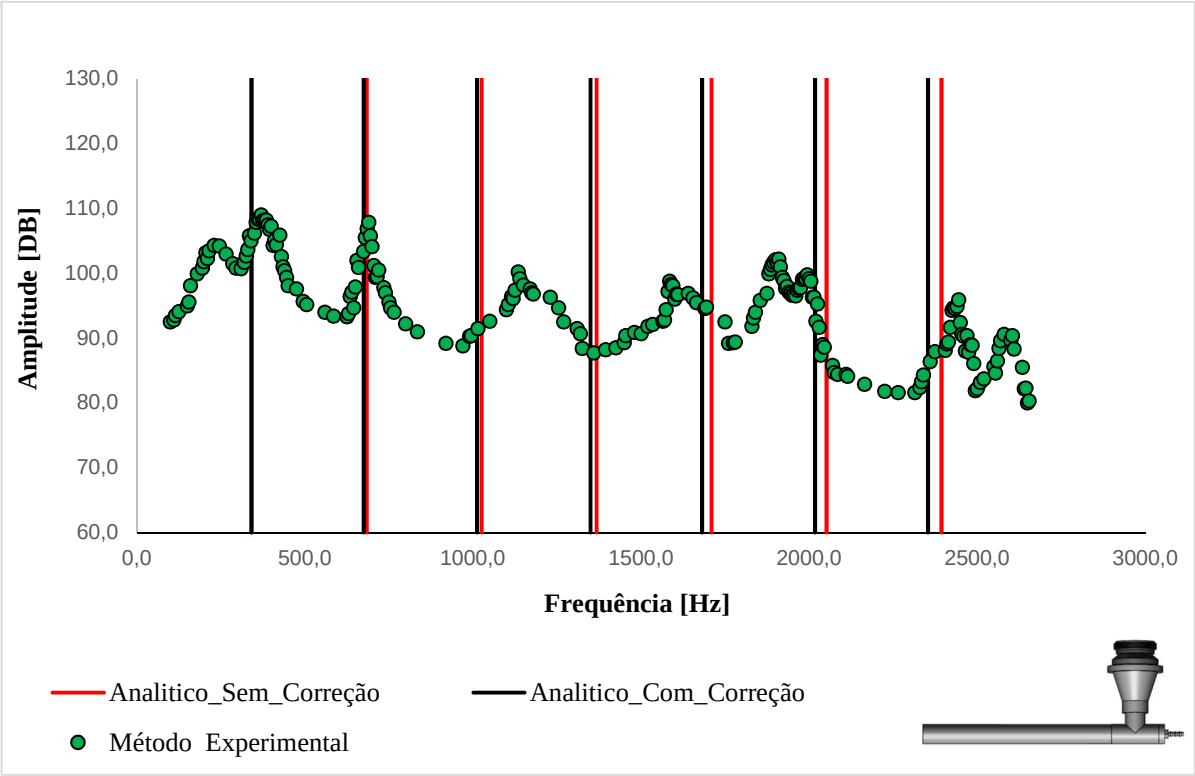

Figure 4. Frequency x amplitude for open-open tube

The results presented in Table 2 show the difference in percentage between the experimental and analytical methods.

Table 2**.** Frequencies and relative errors comparisons

Nº harmonics	Experimental frequency (Hz)	Corrected analytical frequency (Hz)	Experimental x analytical difference (%)
1	370,0	335,1	8,0
2	690,0	670,2	2,2
3	1135,0	1005,4	10,8
4	1585,0	1340,5	14,9
5	1910,0	1675,6	11,9
6	2445,0	2010,8	17,5
7	2605,0	2345,9	9,6

3.1 Numerical results of the combustion

Figure 5a shows the velocity distribution at the burner outlet, where a rapid increase is observed at the output near the diffuser, with a maximum value of 1.107m/s. This velocity increment was due to the geometric shape of the diffuser, providing the expansion of the gas.

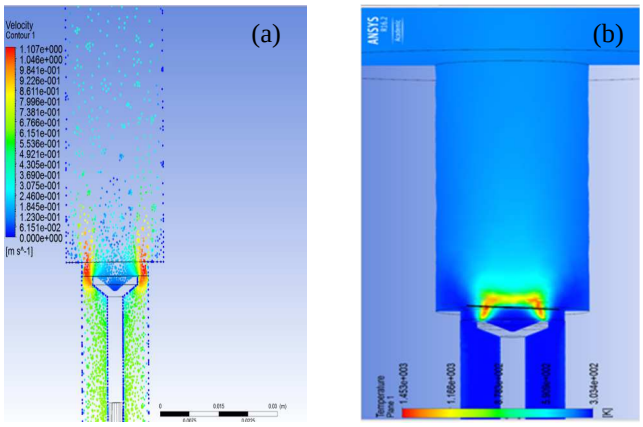

Figure 5. Boundary variables
a) velocity, b) temperature

In Figure 5b, the temperature distribution is higher in the region located just above the diffuser on the anchoring disc, occurring in this region the complete combustion of the gases with heat release. The temperature decreases in the region near the walls of the tube.

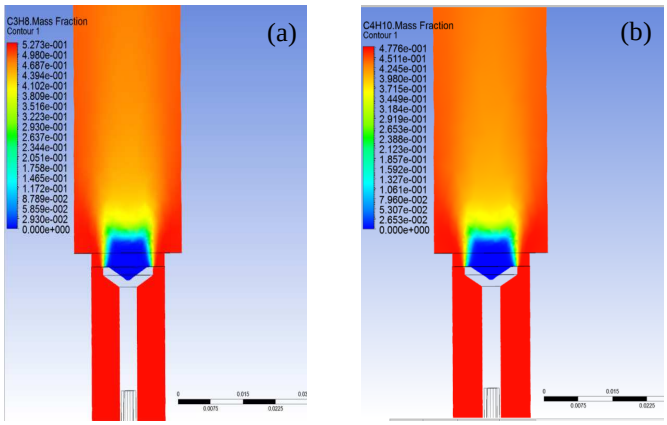

Figure 6. Fractions of pollutants
a) Fractions of Propane, b) fractions of Butane

Figure 6 shows the reduction of the propane and butane mass fractions in the region near the anchor of the burner where combustion occurs.

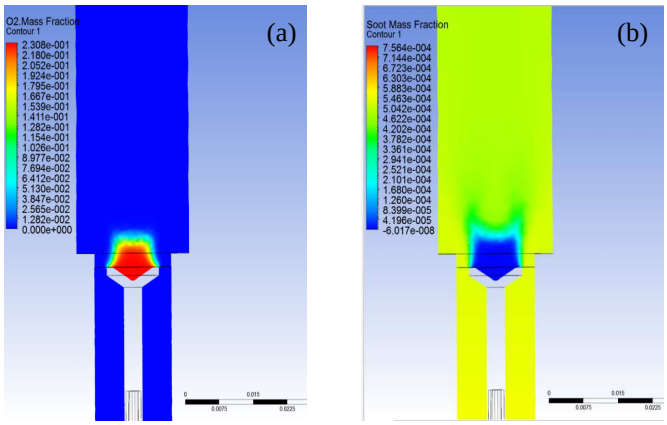

Figure 7. Fractions of oxidants and pollutants
a) fractions of Oxygen, b) fractions of soot

Figure 7a shows an increase in oxygen consumption in the center near the anchoring of the burner due to the occurrence of combustion. Also it is observed in Figure 7b a low soot formation in the anchoring region. The amount of soot increases as the flame moves away from base of the anchor.

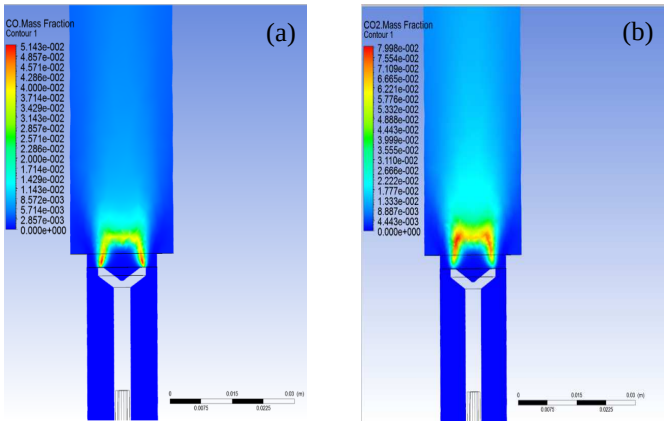

Figure 8. Fractions of pollutants
a) fractions of Carbon Monoxide, b) fractions of Carbon Dioxide

Figure 8 shows the fractions of carbon monoxide and carbon dioxide. An increasing of pollutants is verified in the region near the anchor due to the combustion.

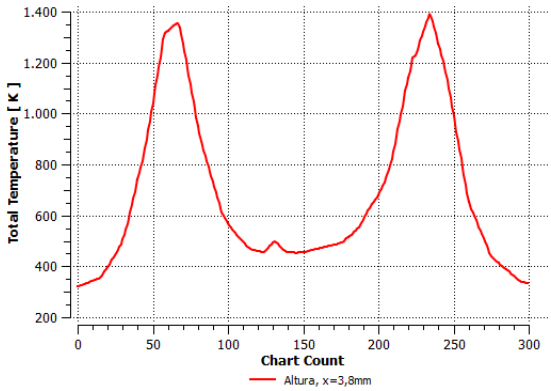

Figure 9. Temperature profile of the flame

Figure 9 shows the numerically obtained graph of the flame's temperature variation at distance of 0.0038m from the anchor of the burner. A notable temperature reduction in the central part of the flame is observed due to the thermal exchange with the cold parts of the walls of the burner.

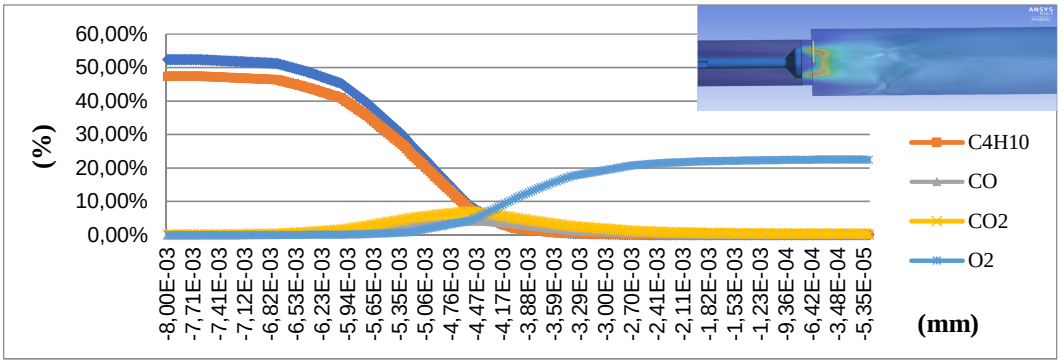

Figure 10. Fraction of mass: gases in combustion

The graph of Figure 10 shows in percentages used in the combustion, where the fractions of propane (C3H8) and butane (C4H10) as they approach radially towards the anchor of the burner flame, their consumption drastically reduces from 50% to approximately 0%, since they are being consumed in the combustion process. It is also observed that there

is an 8% increase in the fractions of carbon monoxide (CO) and carbon dioxide (CO2), products generated from the combustion process. Finally, the curve representing oxygen (O2) increases by more than 20% because the oxidant is being drawn into the combustion and mixed with the fuel (LPG).

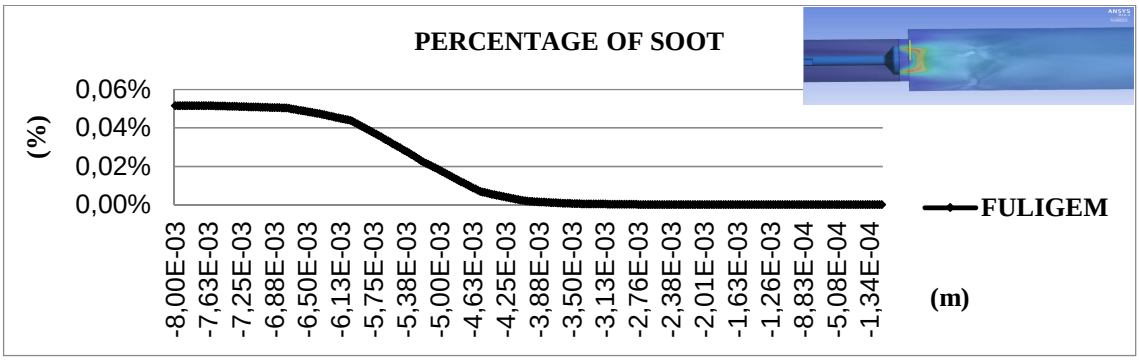

Figure 11. Fraction of mass: soot in the combustion

The graph of Figure 11 shows the percentage of soot emission resulting from the combustion, which drastically reduces from 0.05% to nearly 0% as it radially approximates towards the flame anchoring of the burner. This behavior is desirable because when they approach the center of the flame there is a lower emission of soot due to burning between the oxidant and the fuel being more complete.

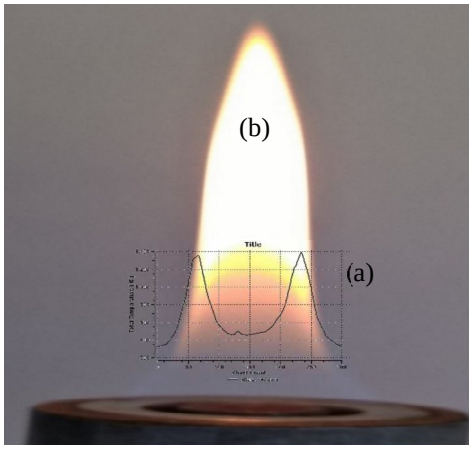

Figure 12. Temperature profile
a) graph of Figure 9, b) laminar diffusion flame

Figure 12 shows the graph of Figure 9 overlapping the flame. They are arranged in an axisymmetric manner, in such a way that the higher temperature occurs at the border of the flame anchoring disc, due to the edge effect of the diffuser. In the center of the flame there is a drastic reduction in temperature. This is because the gas that leaves as a jet from the combustion chamber does not have enough oxygen, therefore the combustion in this region is incomplete and leads to the formation of carbon monoxide.

3.2 Experimental results of the combustion

The recordings of flame behavior of the burner in operation, with the configurations of frequencies coincident with the previously determined acoustic modes, were performed with the aid of a digital camera positioned at a height of 1.15m and distance of 0.20m from the flame. As shown in Table 3, the flames presented yellow-colored luminosity caused by the presence of soot generated during the combustion process.

When acoustic excitation is imposed on the burner's body by a speaker with a voltage amplitude of 0.5V it causes a stirring in the fuel molecules. The excitation frequencies correspond to acoustic modes at frequencies of 370, 690 and 1135Hz as shown in Fig. 3b, 3c and 3d of the Table 3. In these figures is observed the increase in the velocity of the fuel jet, reaching a point where the flame remains at the outlet of the injection point. It is important to note that the phenomenon called *lifted flame* does not occur, ie, an increase in jet velocity to the point where the flame is displaced from the base of the anchor, generating an area with no chemical reaction. Another observation is the presence of vortex in the luminous region of the flame and occurrence of more intense noise. At the base of the flame is notable a reduction of luminosity,

partially losing the yellowish coloration to a bluish coloration, and this phenomenon occurred because of the greater acoustic energy in the utilized frequencies.

The flames evaluated in figures 3e, 3f, 3g and 3h of Table 3, they presented a yellow luminosity and intense brightness with indication of presence of soot and without significant changes in the appearance of the flame.

Table 3 presents the best configuration for burner operation considering the parameters of voltage, flow and pressure, where a lean mixture with low LPG gas consumption occurs and less voltage is imposed to the audio transducer.

Table 3**.** Visual analysis with and without acoustic actuation

AC voltage (V)	Flow (g/s)	Pressure (kgf/cm^2)	Without acoustic actuation	With acoustic actuation						
				1st Frequencies (Hz)	2nd Frequencies (Hz)	3rd Frequencies (Hz)	4th Frequencies (Hz)	5th Frequencies (Hz)	6th Frequencies (Hz)	7th Frequencies (Hz)
0.50 imposed to the speaker	1 % open of valve 0.05	0.25	0 (a)	370 (b)	690 (c)	1135 (d)	1585 (e)	1910 (f)	2445 (g)	2605 (h)
										

4. CONCLUSIONS

The experimental methods allowed the analysis to choose the best burner configuration, considering the criteria of acoustic energy intensity and frequencies. As observed by the experimental method, at low frequency the acoustic transducer produces greater energy with large displacements, and therefore greater capacity of excitation of the gas during the pulse combustion.

For the numerical evaluation through CFD modelling, were defined the main physical quantities involved in the combustion, especially the temperature, whose numerical computational prediction presented a value of 1179 ºC (1453 K), with a difference of 26% when compared to the experimental results identified by Devadiga & Rao (2013). The numerical study also presented a low emission of soot near the anchor and an increase of this pollutant as it moves away from the anchor of the burner.

Finally, it was possible to demonstrate that different acoustic pressure fields reduce the soot emissions during pulsed combustion, and that small-scale improvements can generate significant effects in a non-stop operation. If these improvements are reapplied in other industrial combustion systems, the performance gains may be even greater.

5. REFERENCES

Bastos, V.H. *Investigação de chamas pulsates difusivas livres*. São José dos Campos. Dissertação (Mestrado em Combustão e Propulsão) - Instituto Nacional de Pesquisas Espaciais, 2001. No prelo.

Bowman, C.T., 1992, *"Control of Combustion-Generated Nitrogen Oxide Emissions: Technology Driven by Regulation"*, Proceedings of the Combustion Institute, 24, 859-876.

Carvalho Jr., J. A.; Miller, N.; Daniel B.R.; Zinn B.T. *Combustion characteristics of unpulverized coal under pulsating and non-pulsating conditions. Fuel*, v. 66, n. 1, 1987.

Devadiga, A., Nageswara, R.T.; *"Optimizing Bunsen burner Performance Using CFD Analysis"*. International Journal of Modern Engineering Research (IJMER) 1.3: 2773-2785, 2013.

ISO 3744, *"Acoustics – Determination of sound power levels of noise sources using sound pressure – Engineering methods in na essentially free fiels over a reflecting plane"*, International Organization for Standardization – ISO, 1994.

ISO 3746, *"Acoustics – Determination of sound power levels of noise sources using sound pressure – Survey methods using an enveloping measurement surface over a reflecting plane"*, International Organization for Standardization – ISO, 1995.

Kassem, H. I., et al. *Implementation of the Eddy Dissipation Model of turbulent non-premixed combustion in Open FOAM*. International Communications in Heat and Mass Transfer, v. 38, p. 363-367, 2011.

Moura, T.M., 1981.*Análise numérica dos fenômenos de onda em coletores de admissão de motores de combustão interna*. 2013 Campinas, São Paulo -SP.

Oliveira, F. L. *Presença de Fuligem não Pré-misturadas com Excitação Acústica*. 2007. 97f. Tese de mestrado – Instituto Tecnológico de Aeronáutica, São José dos Campos-SP.

Reis, L.C. B. S. *Análise do escoamento turbulento por um queimador industrial a gás utilizando dinâmica dos fluidos computacional*. 2013. 173. Tese (doutorado) Universidade Estadual Paulista, Faculdade de Engenharia de Guaratinguetá, 2013.

Santos, T. P., et al. *Numerical Modelling of Swirling Diffusive Flames*. Published by EDP Sciences, 2016.

Tipler, P. A. *Física para Cientistas e Engenheiros*, *volume 1*, Rio de Janeiro,ed. LTC ,2012.

Vuolo, J. H. *Fundamentos da Teoria de Erros*. São Paulo,ed. Edgard Blücher,1996.

ZINN, B.T. *Pulsating combustion. In: Advanced Combustion Methods*, ed. F.J. Weinberg, Academic Press. 1986.

6. RESPONSIBILITY NOTICE

The authors are the only responsible for the printed material included in this paper.